

Proteomics of Uterosacral Ligament Connective Tissue from Women with and without Pelvic Organ Prolapse

Xiang-Juan Li, Hai-Tao Pan, Juan-Juan Chen, Yi-Bin Fu, Min Fang, Guo-Hua He, Tao Zhang, Hai-Gang Ding, Bin Yu, Yi Cheng, Ya-Jing Tan, Fa-Lin Zhao, Abraham N. Morse, and He-Feng Huang*

Purpose: Damage to the uterosacral ligaments is an important contributor to uterine and vaginal prolapse. The aim of this study is to identify differentially expressed proteins (DEPs) in the uterosacral ligaments of women with and without pelvic organ prolapse (POP) and analyze their relationships to cellular mechanisms involved in the pathogenesis of POP.

Experimental design: Uterosacral ligament connective tissue from four patients with POP and four control women undergo iTRAQ analysis followed by ingenuity pathway analysis (IPA) of DEPs. DEPs are validated using Western blot analysis.

Results: A total of 1789 unique protein sequences are identified in the uterosacral ligament connective tissues. The expression levels of 88 proteins are significantly different between prolapse and control groups (≥ 1.2 -fold, $p < 0.05$). IPA demonstrates the association of 14 DEPs with “Connective Tissue Function.” Among them, fibromodulin, collagen alpha-1 (XIV) chain, calponin-1, tenascin, and galectin-1 appear most likely to play a role in the etiology of POP.

Conclusions and clinical relevance: At least six proteins not previously associated with the pathogenesis of POP with biologic functions that suggest a plausible relationship to the disorder are identified. These results may be helpful for furthering the understanding of the pathophysiological mechanisms of POP.

1. Introduction

Pelvic organ prolapse (POP) is defined as “the descent of one or more aspects of the vagina and uterus: the anterior vaginal wall, posterior vaginal wall, the uterus (cervix), or the apex of the vagina (vaginal vault or cuff scar after hysterectomy)”.^[1] POP is a common, costly, and debilitating disorder that negatively impacts the quality of life of many women. It has been reported that approximately 3% of women in the United States had symptoms of vaginal bulging;^[2] however, the prevalence of POP identified by pelvic examination was much higher, up to 40–50% in some studies.^[3] Although its symptoms are not life threatening, it is a significant health burden and is associated with a significant economic impact.

The etiology of POP appears to be related to connective tissue genetics and metabolism. Genomic analysis of families with a high penetrance of POP has yielded important insights into the molecular and cellular mechanisms that may be involved in the development of POP.^[4] However, genomic techniques

Dr. X.-J. Li, Dr. Y. Cheng, Dr. H.-F. Huang
Key Laboratory of Reproductive Genetics
Ministry of Education
Zhejiang University
Hangzhou 310058, China
E-mail: hhf57@zju.edu.cn

Dr. Y.-J. Tan, Dr. H.-F. Huang
International Peace Maternity and Child Health Hospital
School of Medicine
Shanghai Jiao Tong University
Shanghai 200240, China


Dr. Y. Cheng
Department of Pathology and Pathophysiology
School of Medicine
Zhejiang University
Hangzhou 310058, China

Dr. X.-J. Li, Dr. J.-J. Chen
Hangzhou Women's Hospital
Hangzhou 310008, China

Dr. H.-T. Pan, Dr. Y.-B. Fu, Prof. M. Fang, Dr. G.-H. He, Dr. T. Zhang
Dr. H.-G. Ding, Dr. B. Yu
Shaoxing Women and Children's Hospital
Shaoxing 312000, China

Dr. A. N. Morse
Guangzhou Women and Children's Medical Center
Guangzhou 510623, China

Prof. F.-L. Zhao
Hangzhou Normal University
Hangzhou 311121, Zhejiang, China

 The ORCID identification number(s) for the author(s) of this article can be found under <https://doi.org/10.1002/prca.201800086>

DOI: 10.1002/prca.201800086

have some limitations when attempting to understand the dynamic relationship of multiple protein functions in normal and affected tissues, and the correlation between mRNA and protein levels is insufficient to predict protein expression levels.^[5] Direct assessment of the proteins involved in a target biological function can be valuable for the understanding of biological systems. Proteomic techniques may elucidate complex patterns of protein expression which can help fill the gap between genomics and phenotypes.^[6] In 2015, Sun et al. analyzed the uterosacral ligament in postmenopausal women with and without POP using 2D gel-based proteomic tools. They identified eight downregulated proteins in the POP group by MALDI-MS.^[7] 2DE has been used for more than 25 years and was the first technique capable of supporting the concurrent quantitative analysis of large numbers of gene products. However, studies have revealed that the dynamic range of 2DE technique is limited.^[8] In addition, some studies have revealed that 2DE identified only the most abundant proteins.^[9]

The aim of this study was to investigate the differential expression of proteins in the uterosacral ligament of women with or without POP, and analyze their relationships to cellular mechanisms already known to be involved in the pathogenesis of POP. We applied HPLC-MS/MS using the iTRAQ analysis method to identify differentially expressed proteins (DEPs) between the two groups. We analyzed the DEPs with respect to molecular function, biological processes, and signaling pathways using ingenuity pathway analysis (IPA). IPA is a knowledge database relying on published literature related to protein function, localization, relevant interactions, and biological mechanisms. Disease analysis, pathway analysis, and network generation can be performed using IPA. HPLC-MS/MS, iTRAQ analysis, and IPA were utilized to investigate the proteomics of the etiology and pathogenesis of POP.

2. Experimental Section

2.1. Clinical Specimen Collection

The study was endorsed by the Hangzhou Women's Hospital Ethics Committee (docket#2015-001-03) and written informed consent was obtained from each subject. Uterosacral ligament tissues were collected during hysterectomy procedures at Hangzhou Women's Hospital (Hangzhou, China) between March and August 2016. The subjects consisted of eight women with stage III or stage IV prolapse based on the POP quantification (POP-Q) examination and eight controls with stage 0–1 prolapse and no history of prolapse surgery. All of the patients were postmenopausal. Patients with a history of connective tissue diseases such as Marfan or Ehlers–Danlos syndromes were excluded. None of the subjects had received any hormonal treatment in the 3 months prior to surgery. Patient demographics and clinical characteristics are presented in **Table 1**. The full thickness specimens were taken from the uterosacral ligaments near their insertion into the cervix. The specimens were 0.5–1 cm long. No specimen had any gross evidence of fracture or other damage. Uterosacral ligament samples were washed in a cold phosphate buffered saline

Clinical Relevance

Damage to the uterosacral ligaments is associated with uterine and apical vaginal prolapse. The cellular and molecular pathogenesis of pelvic organ prolapse (POP) is not well understood. Our iTRAQ analysis demonstrated 14 differentially expressed proteins that were associated with "Connective Tissue Function." Among them, fibromodulin, collagen alpha-1 (XIV) chain, calponin-1, tenascin, and galectin-1 appear most likely to play a role in the etiology of POP. Further investigation of the possible role of these proteins and their associated pathways may help focus further research on the cellular mechanisms of POP.

solution to eliminate blood. Tissue samples were then snap frozen in liquid nitrogen and stored at $-80\text{ }^{\circ}\text{C}$ within 30 min of excision.

2.2. Protein Extraction and Digestion

A total of 0.1 mg of each ligament tissue sample was ground into a powder in liquid nitrogen and homogenized in extraction buffer (4% SDS, 1 mM DTT, and 150 mM Tris-HCl, pH 8.0). Protein extraction was performed by cell lysis buffer at $95\text{ }^{\circ}\text{C}$ for 5 min, followed by sonication on ice. The crude extract was then incubated at $95\text{ }^{\circ}\text{C}$ again and cleared by centrifugation at $14\ 000 \times g$ for 30 min at $15\text{ }^{\circ}\text{C}$. Thereafter, the supernatant was collected and the protein concentration was measured by the BCA protein assay reagent from Pierce (Pierce, Rockford, IL, USA).

Protein digestion was performed using the filter-aided sample preparation (FASP) method as previously described.^[10] Briefly, 200 μg of total protein samples were diluted in 30 μL of solution including 4% SDS, 100 mM Tris-HCl pH 8.0, and 100 mM dithiothreitol, and were heated at $95\text{ }^{\circ}\text{C}$ for 5 min. After each sample was cooled to room temperature, the sample was loaded onto an ultrafiltration filter (cutoff 10 kDa, Sartorius, Goettingen, Germany). Two hundred microliters of UT buffer (8 M urea and 150 mM Tris-HCl, pH 8.0) was added to the filter and centrifuged it at $14\ 000 \times g$ at $20\text{ }^{\circ}\text{C}$ for 30 min. Subsequently, 100 μL of iodoacetamide solution (50 mM iodoacetamide in UT buffer) was added for blocking reduced cysteines and the samples were incubated for 20 min in darkness. Then the filters were centrifuged at $14\ 000 \times g$ at $20\text{ }^{\circ}\text{C}$ for 20 min. The filters were washed with 100 μL UT buffer at $14\ 000 \times g$ for 20 min. This step was repeated twice. Then, 100 μL dissolution buffer (AB Sciex, Framingham, MA, USA) was added to the filter and it was centrifuged at $14\ 000 \times g$ at $20\text{ }^{\circ}\text{C}$ for 30 min and this step was repeated twice. Finally, 40 μL of trypsin (Promega, Madison, WI, USA) buffer (2 μg trypsin in 40 μL dissolution buffer) were added and the samples were digested overnight at $37\text{ }^{\circ}\text{C}$. Each filter unit was transferred to a new tube and centrifuged at $14\ 000 \times g$ at $20\text{ }^{\circ}\text{C}$ for 30 min. The resulting peptide concentrations were estimated by UV light spectral density at OD_{280} .

Table 1. Comparison of characteristics between the two groups.

Items	Control			Experiment			t/Z Value	p-Value
	n	$\bar{x} \pm s$	M	n	$\bar{x} \pm s$	M		
Age	8	63.25 ± 8.03	64.50	8	64.63 ± 8.33	64.00	−0.336	0.742
BMI	8	25.58 ± 3.34	25.55	8	23.19 ± 2.40	23.65	1.646	0.122
Age of menopause	8	50.00 ± 3.93	49.50	8	51.25 ± 1.58	51.50	−0.835 ^{a)}	0.425
FSH	8	47.41 ± 23.87	47.60	8	57.48 ± 15.26	57.55	−1.005	0.332
LH	8	18.83 ± 10.30	19.88	7	24.15 ± 8.13	20.79	0.400 ^Δ	0.442
E2	8	41.50 ± 61.88	18.50	8	23.63 ± 14.44	19.50	0.875 ^Δ	0.878
T	8	0.25 ± 0.07	0.28	8	0.28 ± 0.20	0.24	0.343 ^Δ	0.382
P	8	2.30 ± 5.04	0.71	8	0.49 ± 0.33	0.46	0.400 ^Δ	0.442
Glucose	8	5.21 ± 1.21	4.85	8	4.86 ± 0.51	4.81	0.674 ^Δ	0.721
Hb	8	121.13 ± 10.74	120.50	8	129.71 ± 14.56	135.00	−1.313	0.212
Parity	8	2.38 ± 1.06	2.50	8	1.88 ± 0.99	2.00	0.296 ^Δ	0.328

^{a)} Equal variances not assumed, adjusted t-test is used, ^Δ normal distribution not assumed, Wilcoxon test is used.

2.3. Protein Digestion and iTRAQ Labeling

The resulting peptide mixture was labeled using the 8-plex iTRAQ reagent according to the manufacturer's instructions (AB Sciex, Framingham, MA, USA). The four control group (C) samples were labeled with mass 113, 114, 115, and 116 isobaric tags, while the four samples from the POP group were labeled with mass 117, 118, 119, and 121 isobaric tags. The labeling solution was incubated at room temperature for 2 h before further analysis.

2.4. Strong Cationic-Exchange Chromatography Fractionation

The combined sample was acidified with 1% trifluoroacetic acid before being subjected to strong cationic-exchange chromatography (SCX) fractionation using a PolySULFOETHYL column (4.6 × 100 mm, 5 μm, 200 Å, Poly LC Inc., Columbia, MD, USA). Solvent A consisted of 10 mM KH₂PO₄ in 25% v/v ACN, and solvent B was solvent A with 500 mM KCl added. The solvents were applied using a gradient of 0–10% solvent B for 2 min, 10–20% solvent B for 25 min, 20–45% solvent B for 5 min, and 50–100% solvent B for 5 min. The elution was monitored by absorbance at 214 nm and fractions were collected every 1 min. Finally, these samples were combined into ten fractions based on the quantity of peptide and then desalted on C18 cartridges (Sigma, Steinheim, Germany). Each SCX salt step fraction was dried in a vacuum centrifuge and reconstituted with 40 μL 0.1% v/v trifluoroacetic acid.

2.5. LC-ESI-MS/MS Analysis

A volume of 5 μg of peptide mixture from each fraction was subjected to nano LC-MS/MS analysis. Peptide mixtures were loaded onto the Thermo EASY-nLC column (Thermo Finnigan, San Jose, CA, USA) (100 mm × 75 μm, 3 μm) in solvent C (0.1% formic acid) and separated with a linear gradient of solvent D (80% acetonitrile with 0.1% v/v formic acid) at a flow rate of

300 nL min^{−1} over 120 min: 0–100 min with 0–45% solvent D; 100–108 min with 45–100% solvent D; 108–120 min with 100% solvent D.

The Q-Exactive (Thermo Finnigan, San Jose, CA, USA) mass spectrometer acquired data in the positive ion mode, with a selected mass range of 300–800 mass/charge (*m/z*) ratio. Dynamic exclusion was used with 40.0 s duration. Q-Exactive survey scans were set as 70 000 at *m/z* 200 and 17 500 at *m/z* 200 of resolution for HCD spectra. MS/MS data were acquired using a data-dependent acquisition method using the top ten most abundant precursor ions. The normalized collision energy was 30 eV and the underfill ratio was defined as 0.1% on the Q-Exactive.

2.6. Protein Identification and Quantification

Protein identifications were performed using the MASCOT search engine (version 2.2.1; Matrix Science, London, UK) embedded into Proteome Discoverer 1.3 (Thermo Electron, San Jose, CA, USA), searching against the Uniport database of human protein sequences (03-2013, 133 549 entries, downloaded from: <http://www.uniprot.org/>) and the decoy database. Search parameters were set as follows: monoisotopic mass, peptide mass tolerance at ±20 ppm and fragment mass tolerance at 0.1 Da, trypsin as the enzyme, and allowing up to two missed cleavages. Variable modifications were defined as oxidation of methionine and iTRAQ 8-plex labeled tyrosine while lysine and N-term of peptides labeled by iTRAQ 8-plex and carbamidomethylation on cysteine were specified as fixed modifications. False discovery rate (FDR) of both protein and peptide identification was set to be less than 0.01. Protein identification was supported by at least one unique peptide identification.

2.7. Western Blot

For Western blot analysis, the protein samples of uterosacral ligament were prepared from four control subjects and four

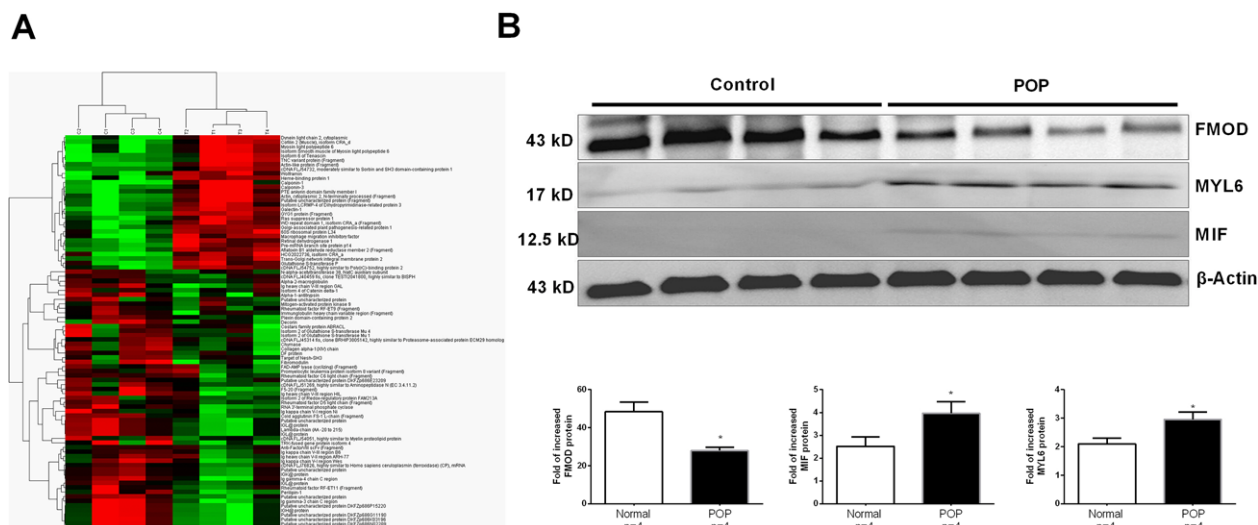


Figure 1. A) Hierarchical clustering of significant differentially expressed proteins in uterosacral ligament tissue. The bright red color indicates upregulation, the deep green color indicates downregulation, and black portrays no change. B) Validation of the differential expression of three selected proteins by Western blot analysis: FMOD, MYL6, and MIF. Data are presented as mean \pm SD ($n = 4$). $p < 0.05$ compared to the corresponding controls.

POP patients. Human uterosacral ligament sample was homogenized in 500 μ L 1 \times RIPA buffer containing protease inhibitors (1 μ g mL⁻¹ leupeptin and 1 μ g mL⁻¹ phenylmethylsulfonyl fluoride). Samples were loaded at 30 μ g per lane and separated in a 10% SDS gel. The separated samples were transferred to a nitrocellulose membrane (Bio-Rad, Hercules, CA, USA). After incubating for 1 h with blocking buffer, the membrane was incubated overnight at 4 $^{\circ}$ C with primary antibodies against fibromodulin (FMOD) (Abcam ab226934, Cambridge, UK; 1:1000), MYL6 (Abcam ab174169, Cambridge, UK; 1:1000), MIF (Abcam ab187064, Cambridge, UK; 1:1000), and β -actin (Santa Cruz Biotechnology sc1616, Santa Cruz, CA, USA; 1:1000). After three washes with 1 \times TBST, pH 7.4, each membrane was incubated with the appropriate secondary antibody (1:1000) at room temperature for 1 h. After additional three washes, protein intensities were visualized with the ECL detection system (Beyotime, Beijing, China).

2.8. Bioinformatics Analysis

IPA (www.ingenuity.com, Qiagen, Hilden, Germany) included a manually annotated database of protein interactions and metabolic reactions obtained from scientific literature. Gene names of all identified proteins and their corresponding mean fold change values were imported into IPA and processed using the shortest path algorithm. The IPA generated a rank order of significance of protein association.

2.9. Statistical Analysis

All the statistical analyses of this study were carried out using Prism 6 from GraphPad (San Diego, CA, USA). Statistical significance for comparison of baseline group characteristics was determined by using appropriate non-parametric tests. All samples

were tested in triplicate, and the data are expressed as means \pm SD. $p < 0.05$ was considered significant.

2.10. Data Availability

The mass spectrometry proteomics data have been deposited to the ProteomeXchange Consortium via the PRIDE^[11] partner repository with the dataset identifier PXD011467 (<https://doi.org/10.6019/PXD011467>).

3. Results

3.1. Protein Profiles of Ligament Tissue

In this study, the two groups appeared similar with respect to age, age at menopause, and body mass index. Using untargeted proteomic analysis, we identified 1789 non-redundant proteins (Table 1, Supporting Information) in human uterosacral ligament with high confidence (one or more unique peptides with an FDR less than 1%). Among them, 88 proteins were found to be differentially expressed using the threshold of (≥ 1.2 -fold, $p < 0.05$) (Table 2, Supporting Information), including 30 upregulated proteins and 58 downregulated proteins in the samples from subjects with prolapse. The hierarchical clustering of these DEPs is visualized in a heat map (Figure 1A).

3.2. Western Blot Validation

After the iTRAQ analysis, we performed Western blot analysis to verify three of the most interesting DEPs discovered by iTRAQ analysis. Western blot demonstrated statistically significant changes in FMOD, MYL6, and MIF expression in the uterosacral ligaments of women with POP (Figure 1B). The direction and magnitude of differential expression were consistent

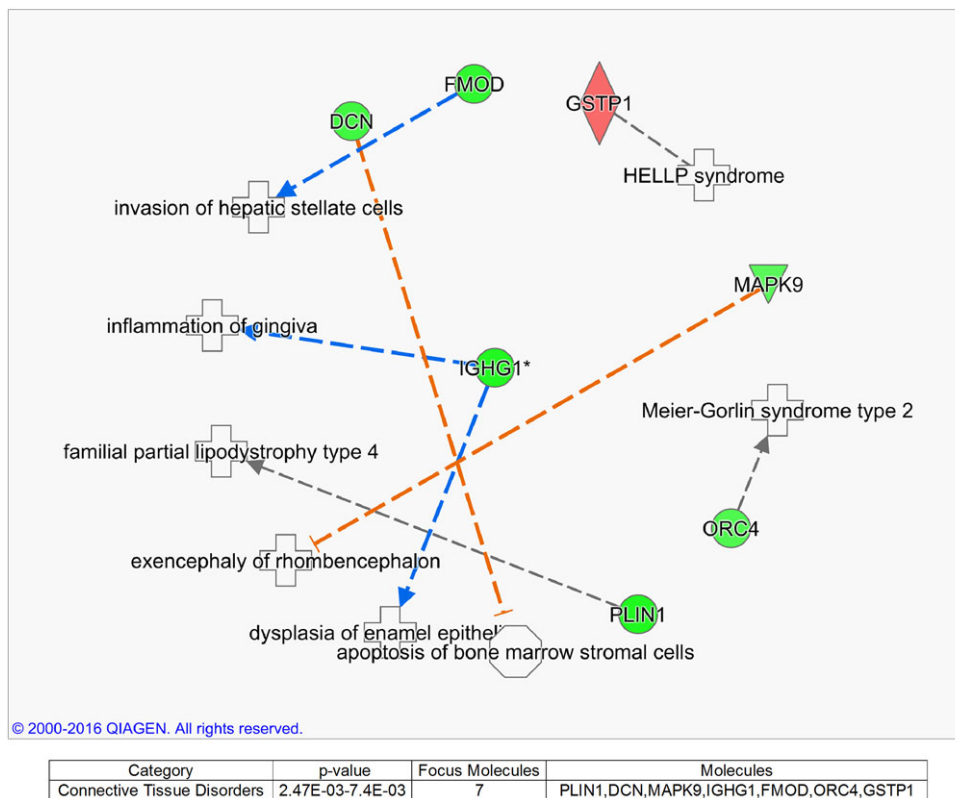


Figure 2. Downstream effect analysis of specific differentially expressed proteins associated with “Connective Tissue Disorders” by the iterative ingenuity pathway analysis. For this developmental disease network, genes or gene products are represented as *nodes*, and the biological relationship between two nodes is represented as an *edge*. All edges are supported by at least one publication as stored in the Ingenuity Knowledge database. The intensity of the node color indicates the degree of up- (red) or down- (green) regulation.

with the iTRAQ analysis results. Because several DEPs were related to “Connective Tissue Function,” we further analyzed the association of these proteins with Connective Tissue Function (Figure 3).

3.3. Disease and Function Analysis

All 88 DEPs were further analyzed by IPA, and these DEPs clustered in subcategories of “Disease and Disorder” and in “Physiological System Development and Functions.” According to the overlapping *p*-values, these DEPs were significantly related to 28 subcategories of “Disease and Disorder” (Figure 1, Supporting Information) and 27 subcategories of “Physiological System Development and Functions” (Figure 2, Supporting Information). Accordingly, based on “Disease and Disorder” analysis of the gene list, 7 DEPs were associated with “Connective Tissue Disorders” (Figure 2), and based on “Physiological System Development and Functions” analysis, 14 DEPs were associated with “Connective Tissue Function” (Figure 3).

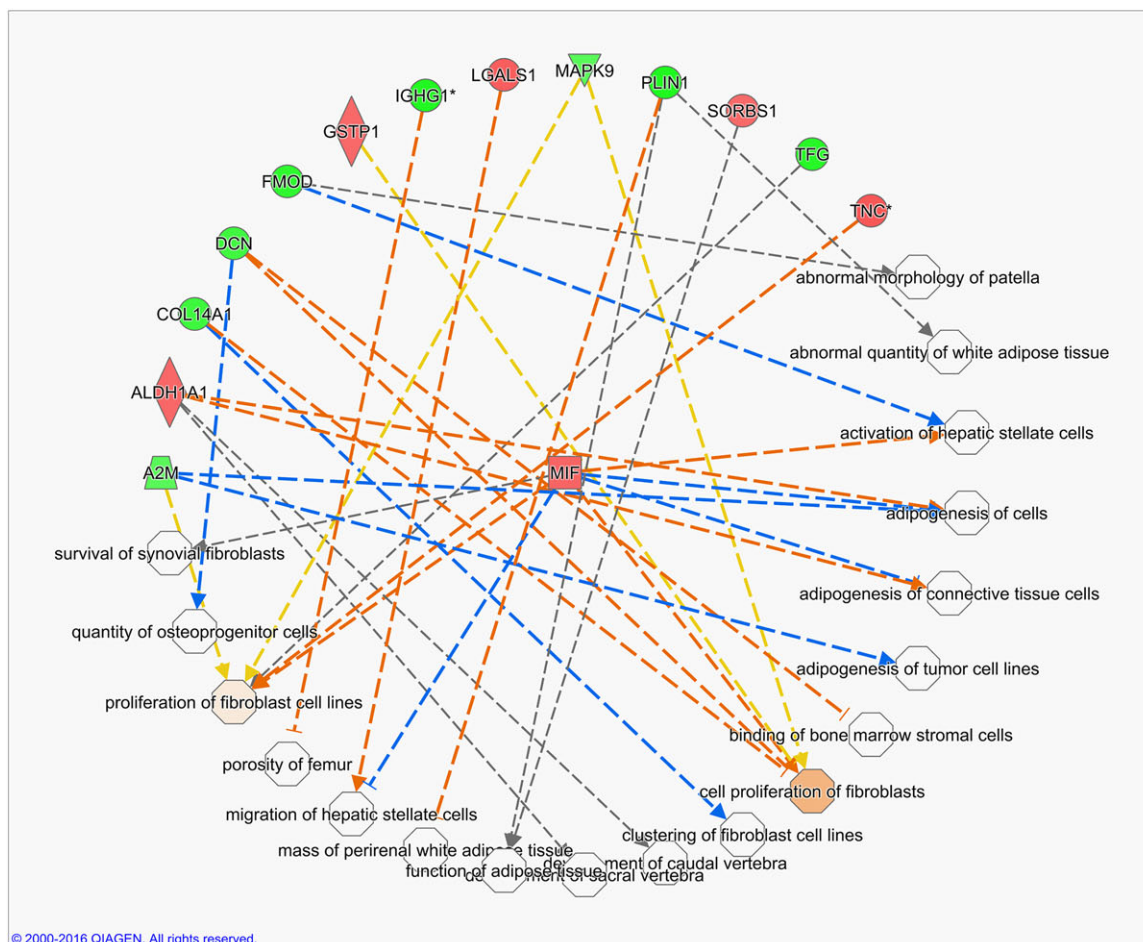
3.4. Network Analysis

To better understand the potential roles of these DEPs, the data were further analyzed using network analysis. Hypothetical

networks were built between the experimentally found proteins and the IPA database proteins. The relevant pathway maps were then prioritized according to their statistical significance ($p < 0.001$) and networks were graphically visualized as hubs (proteins) and edges (the relationship between proteins). The best matching network involved 17 DEPs. It was associated with the IPA functions including “Drug Metabolism,” “Protein Synthesis,” and “Small Molecule Biochemistry” (Figure 3, Supporting Information).

4. Discussion

Proteomics complements other functional and genomic approaches for understanding the physiology and pathophysiology of diseases. Integration of these datasets can improve our understanding of both gene regulation and downstream protein function. In this study, we generated a proteome profile of human uterosacral ligament tissue in women with or without POP using iTRAQ methodology and identified a set of DEPs unique in comparison to a previous study using MALDI-MS methodology.^[7] Because the methodology is different from MALDI-MS, it is not surprising that the DEPs identified in our study were different from the previous analysis of uterosacral ligament.^[7] We used IPA to further analyze the potential biologic significance of DEPs, in terms of possible downstream effects and upstream



Diseases or Functions Annotation	p-Value	Activation z-score	Molecules
cell proliferation of fibroblasts	4.49E-03	0.668	COL14A1,DCN,GSTP1,MAPK9,MIF
proliferation of fibroblast cell lines	9.99E-03	0.175	A2M,MAPK9,MIF,TFG,TNC
adipogenesis of cells	2.97E-03		A2M,ALDH1A1,MIF
migration of hepatic stellate cells	1.34E-03		LGALS1,MIF
function of adipose tissue	4.40E-03		PLIN1,SORBS1
adipogenesis of connective tissue cells	5.07E-03		ALDH1A1,MIF
activation of hepatic stellate cells	6.03E-03		FMOD,MIF
development of caudal vertebra	4.94E-03		ALDH1A1
porosity of femur	4.94E-03		IGHG1
binding of bone marrow stromal cells	7.40E-03		DCN
development of sacral vertebra	7.40E-03		ALDH1A1
survival of synovial fibroblasts	7.40E-03		MIF
adipogenesis of tumor cell lines	9.85E-03		A2M
clustering of fibroblast cell lines	9.85E-03		COL14A1
mass of perirenal white adipose tissue	9.85E-03		PLIN1
abnormal quantity of white adipose tissue	1.47E-02		PLIN1

Figure 3. Downstream effect analysis of specific differentially expressed proteins associated with “Connective Tissue Function” by the iterative ingenuity pathway analysis. For this “Connective Tissue Function” network, genes or gene products are represented as *nodes*, and the biological relationship between two nodes is represented as an *edge*. All edges are supported by at least one publication as stored in the Ingenuity Knowledge database. The intensity of the node color indicates the degree of up- (red) or down- (green) regulation.

regulators, which has provided useful insights into the pathobiology of POP.

Using the “disease and disorders” network IPA we found seven DEPs associated with “Connective Tissue Disorders.” In “Function analysis,” 14 DEPs are involved in “Connective Tissue

Development and Function.” We believe that the most promising DEPs for further investigation regarding their potential involvement in the pathobiology of POP are: collagen alpha-1 (XIV) chain (COL14A1), fibromodulin (FMOD, calponin-1 (CNN-1), tenascin (TNC), and galectin-1 (LGALS1). COL14A1 plays a

role in integrating collagen bundles. It is probably associated with the surface of interstitial collagen fibrils.^[12] FMOD affects the rate of fibril formation and may have a primary role in collagen fibrillogenesis.^[13] CNN-1 is a smooth muscle thin filament-associated protein that is implicated in the regulation and modulation of smooth muscle contraction. It is capable of binding to actin, calmodulin, troponin C, and tropomyosin.^[14] The interaction of calponin with actin inhibits the actomyosin Mg-ATPase activity.^[15] TNC is implicated in the guidance of migrating neurons as well as axons during development, as well as neuronal regeneration. TNC promotes neurite outgrowth from cortical neurons grown on a monolayer of astrocytes.^[16] Stimulation via mechanical stretch may promote the synthesis of TNC and bone marrow stromal cell (BMSC) differentiation into pelvic ligament fibroblasts.^[17] LGALS1 plays a role in regulating apoptosis, cell proliferation, and cell differentiation. Lectin that binds beta-galactoside and a wide array of complex carbohydrates may inhibit CD45 protein phosphatase activity and therefore induces the dephosphorylation of Lyn kinase.^[18] In addition, MYL6 and MIF may also play an important role in the pathogenesis of POP. MYL6 is a regulatory light chain of myosin. Myosin regulatory light chains are required to maintain the stability of myosin II and cellular integrity.^[19] Migration inhibitory factor (MIF) is a proinflammatory cytokine involved in the innate immune response to bacterial pathogens. The expression of MIF at sites of inflammation suggests a role as mediator in regulating the function of macrophages in host defense.^[20]

We also employed IPA Upstream Regulator Analysis to identify upstream regulators that may be involved in the regulation of these candidate proteins. In the upstream analysis, MGEA5, miR-3121-5p, miR-22-3p, and miR-344a-5p were predicted to be in an inhibited state in the women with POP, and TGFB1, miR-4690-5p, miR-4640-5p, and miR-4512 were predicted to be in an activated state. Beta-estradiol may play a regulatory role for FMOD that was predicted to be in an activated state, suggesting a mechanism whereby beta-estradiol may affect the pathogenesis of POP.

Compared with MALDI-MS and 2DE methodology, the iTRAQ method used in the present study has superior breadth and precision in identification of DEPs, and iTRAQ analysis can provide relative quantification simultaneously with the process of generating peptide sequences. We identified more candidate DEPs in the uterosacral ligament of women with POP than those identified in the previous published reports by using MALDI-MS and 2DE.^[7] We demonstrated that 14 DEPs were associated with "Connective Tissue Function" using IPA which is encouraging. However, our study also has some weaknesses. All mass spectrometry analysis methods have significant potential for false-positives, therefore additional confirmatory testing is required to increase confidence in the iTRAQ analysis results. In addition, this investigation only showed the association of the change in protein abundance with POP that does not allow us to understand whether these DEPs are a cause or effect of prolapse. Studies at the organism level, for instance, the production of transgenic mice, will help us to clarify roles of these DEPs in the cellular pathogenesis and development of POP.

In conclusion, by using iTRAQ methodology, 21 DEPs were identified in the uterosacral ligament of women with POP. IPA analysis showed that five DEPs might be more likely to be

associated with biologically plausible areas of connective tissue function and disease. Further investigation of the candidate proteins we identified in this study may expand our understanding of the pathological processes underlying POP.

Supporting Information

Supporting Information is available from the Wiley Online Library or from the author.

Acknowledgements

X.-J.L. and H.-T.P. contributed equally to this work. H.-T.P. has received funding from National Natural Science Foundation of China (No. 81701522), Science Technology Department of Zhejiang Province, China (No.2018C37102, LGF19H040004), and Medical and Health Project of Zhejiang Province, China (Nos.2017KY669, 2019RC296, 2019KY229, 2019KY230). X.-J.L. has received funding from National Natural Science Foundation of Zhejiang Province, China (Nos.LS16H040001, LY19H040002), Medical and Health Project of Hangzhou, China (No.2015A45), Science Technology Department of Hangzhou, China (Nos. 20150633B25, 20150733Q35); Traditional Chinese Medicine Project of Zhejiang Province, China (No.2015ZA168); and China Preventive Medicine Association (No.201811038). T.Z. has received funding from National Natural Science Foundation of Zhejiang Province, China (Nos. LY15H040001, LY16H040008); Science Technology Department of Zhejiang Province, China (Nos. 2016C33222, 2016C33223), and Medical and Health Project of Zhejiang Province, China (No. 2019KY717). **The authors also thank the Shanghai Bioprofile Technology Co., Ltd., for technical assistance.**

Conflict of Interest

The authors declare no conflict of interest.

Keywords

ingenuity pathway analysis, iTRAQ analysis, molecular pathogenesis, musculoskeletal system, pelvic organ prolapse, reproductive system, uterosacral ligament

Received: June 3, 2018
Revised: November 4, 2018
Published online:

- [1] International Urogynecological Association; International Continence Society, B. T. Haylen, D. de Ridder, R. M. Freeman, S. E. Swift, B. Berghmans, J. Lee, A. Monga, E. Petri, D. E. Rizk, P. K. Sand, G. N. Schaer, *Neurourol. Urodyn.* **2010**, *29*, 4.
- [2] J. M. Wu, C. P. Vaughan, P. S. Goode, D. T. Redden, K. L. Burgio, H. E. Richter, A. D. Markland, *Obstet. Gynecol.* **2014**, *123*, 141.
- [3] M. D. Barber, C. Maher, *Int. Urogynecol. J.* **2013**, *24*, 1783.
- [4] J. M. Wu, R. M. Ward, K. L. Allen-Brady, T. L. Edwards, P. A. Norton, K. E. Hartmann, E. R. Hauser, D. R. Velez Edwards, *Am. J. Obstet. Gynecol.* **2013**, *208*, 360.
- [5] S. P. Gygi, Y. Rochon, B. R. Franza, R. Aebersold, *Mol. Cell Biol.* **1999**, *19*, 1720.

- [6] M. Vidal, D. W. Chan, M. Gerstein, M. Mann, G. S. Omenn, D. Tagle, S. Sechi, P. Workshop, *Clin. Proteomics* **2012**, 9, 6.
- [7] Z. J. Sun, L. Zhu, J. H. Lang, Z. Wang, S. Liang, *Chin. Med. J.* **2015**, 128, 3191.
- [8] a) R. Aebersold, M. Mann, *Nature* **2003**, 422, 198; b) N. L. Anderson, J. P. Hofmann, A. Gemmill, J. Taylor, *Clin. Chem.* **1984**, 30, 2031.
- [9] a) S. P. Gygi, G. L. Corthals, Y. Zhang, Y. Rochon, R. Aebersold, *Proc. Natl. Acad. Sci. USA* **2000**, 97, 9390; b) S. R. Pennington, M. R. Wilkins, D. F. Hochstrasser, M. J. Dunn, *Trends Cell Biol.* **1997**, 7, 168.
- [10] a) H. T. Pan, M. X. Guo, Y. M. Xiong, J. Ren, J. Y. Zhang, Q. Gao, Z. H. Ke, G. F. Xu, Y. J. Tan, J. Z. Sheng, H. F. Huang, *J. Proteomics* **2015**, 112, 262; b) H. T. Pan, H. G. Ding, M. Fang, B. Yu, Y. Cheng, Y. J. Tan, Q. Q. Fu, B. Lu, H. G. Cai, X. Jin, X. Q. Xia, T. Zhang, *Placenta* **2018**, 61, 1; c) J. R. Wisniewski, A. Zougman, N. Nagaraj, M. Mann, *Nat. Methods* **2009**, 6, 359.
- [11] J. A. Vizcaino, A. Csordas, N. del-Toro, J. A. Dianes, J. Griss, I. Lavidas, G. Mayer, Y. Perez-Riverol, F. Reisinger, T. Ternent, Q. W. Xu, R. Wang, H. Hermjakob, *Nucleic Acids Res.* **2016**, 44, D447.
- [12] A. V. September, M. Posthumus, L. van der Merwe, M. Schwellnus, T. D. Noakes, M. Collins, *Int. J. Sports Med.* **2008**, 29, 257.
- [13] a) C. S. Li, P. Yang, K. Ting, T. Aghaloo, S. Lee, Y. Zhang, K. Khalilnejad, M. C. Murphy, H. C. Pan, X. Zhang, B. Wu, Y. H. Zhou, Z. Zhao, Z. Zheng, C. Soo, *Biomaterials* **2016**, 83, 194; b) E. J. Lee, A. T. Jan, M. H. Baig, J. M. Ashraf, S. S. Nahm, Y. W. Kim, S. Y. Park, I. Choi, *FASEB J.* **2016**, 30, 2708.
- [14] R. Liu, J. P. Jin, *Gene* **2016**, 585, 143.
- [15] L. J. Bock, C. Pagliuca, N. Kobayashi, R. A. Grove, Y. Oku, K. Shrestha, C. Alfieri, C. Golfieri, A. Oldani, M. Dal Maschio, R. Bermejo, T. R. Hazbun, T. U. Tanaka, P. De Wulf, *Nat. cell Biol.* **2012**, 14, 614.
- [16] a) H. Fu, Y. Tian, L. Zhou, D. Zhou, R. J. Tan, D. B. Stolz, Y. Liu, *J. Am. Soc. Nephrol.* **2017**, 28, 785; b) A. Faissner, L. Roll, U. Theocharidis, *Mol. Cell. Neurosci.* **2017**, 81, 22.
- [17] B. Zhao, M. Hu, H. Wu, C. Ren, J. Wang, S. Cui, *Mol. Med. Rep.* **2017**, 15, 2465.
- [18] a) M. Tang, J. You, W. Wang, Y. Lu, X. Hu, C. Wang, A. Liu, Y. Zhu, *Reprod. Sci.* **2017**, 1933719117725816; b) M. H. Kim, W. H. Wu, J. H. Choi, J. H. Kim, J. H. Jun, Y. Ko, J. H. Lee, *Wound Repair Regen.* **2017**, Suppl 1, S9.
- [19] I. Park, C. Han, S. Jin, B. Lee, H. Choi, J. T. Kwon, D. Kim, J. Kim, E. Lifirsu, W. J. Park, Z. Y. Park, D. H. Kim, C. Cho, *Biochem. J.* **2011**, 434, 171.
- [20] L. Schindler, N. Dickerhof, M. B. Hampton, J. Bernhagen, *Redox Biol.* **2018**, 15, 135.